

Selectivity of cholesterol-imprinted system on self-assembled monolayer

Min Jae Shin* and Young Jae Shin**,[†]

*Department of Cosmetics and Biotechnology, Semyung University, Jecheon, Chungbuk 27136, Korea

**Center for Functional Nanomaterials, Brookhaven National Laboratory, Upton, NY 11973, USA

(Received 2 October 2019 • accepted 19 November 2019)

Abstract—Molecular imprinting was conducted on a thin polymeric membrane stacked on the self-assembled monolayer of a gold plate. The covalent bonding method was used in the molecular imprinting process. Cholesterol was used as a target molecule. Coating with poly(methyl methacrylate) was followed by hydrolysis and extraction of cholesterol. The remaining site was used to recognize cholesterol. Using the cholesterol-imprinted gold electrode as a working electrode, the cholesterol recognition ability was estimated. Various cholesterol analogs were used to obtain the comparative data to determine the imprinting and selectivity factors. The results showed that molecular similarity was important to enhance the recognition. However, the presence of a hydroxyl functional group played a key role in enhancing the molecular recognition, suggesting that molecular polarity and hydrophobicity are important factors.

Keywords: Sensor, Molecular Imprinting Polymer, Cholesterol, Self-assembled Monolayer

INTRODUCTION

Cholesterol is a very important compound in the body; however, excessive cholesterol levels are a serious challenge for health and well-being [1]. During a medical examination, the cholesterol concentrations must be evaluated to ensure healthy levels. High density lipoprotein (HDL) cholesterol and low density lipoprotein (LDL) cholesterol are assessed during the examination. HDL cholesterol is known as good cholesterol, and LDL cholesterol is known as bad cholesterol. Therefore, many studies have attempted to develop systems for the detection of cholesterol, and efforts to develop improved systems for cholesterol detection are ongoing [2-8].

Molecular imprinting is a research technique designed to mimic biological systems such as enzymes [9]. Until now, studies had shown that the performance of the molecular imprinted material is inferior to the biological system [9]. However, a molecular imprinting system can overcome the limitations of the biological system. For example, the biological system can be used under limited conditions of temperature, solvent, and pH, whereas the molecular imprinted system can be used under any conditions of temperature, solvent, and pH [10-14].

Generally, molecular imprinting entails polymerization of the crosslinkable monomer with the target molecule to fabricate a three-dimensional crosslinked polymer [9]. The obtained polymer is ground to fine powder, and many target molecules are placed at the surface of the ground polymeric materials. These target molecules are extracted, and the remaining sites are used to recognize the target molecule. Because the grinding occurs randomly during the molecular imprinting, the target molecule occupies a random position after grinding. If the target molecule is located excessively

shallow beneath the surface, a good molecular imprinted site cannot be obtained. If the target molecule is located excessively deep beneath the surface, the target molecule cannot be extracted. Only the target molecule located at an optimum depth provides a good molecular imprinted site. Therefore, to ensure adequate molecular recognition, surface molecular imprinting was conducted without the grinding process. Nevertheless, ensuring the optimum position of the target molecule is still a challenge [15-22].

Previously, we conducted molecular imprinting at the self-assembled monolayer (SAM) as an extreme case of surface molecular imprinting [23-25]. We found that molecular imprinting at the SAM was effective but still associated with a few limitations. To overcome this, molecular imprinting was conducted at the thin polymeric membrane on SAM [26,27]. In this study, we developed a cholesterol imprinted system at the thin polymeric membrane on SAM and estimated the selectivity to seven cholesterol analogs. Surface molecular imprinting was conducted without the grinding process in this study.

EXPERIMENTAL

1. Materials and Instruments

Poly(methyl methacrylate) (PMMA) (M_w 350,000), cholesteryl chloroformate, benzenethiol, 4-mercaptophenol, triethylamine, potassium ferricyanide [$K_3Fe(CN)_6$], sodium perchlorate, cholesterol, cholic acid, deoxycholic acid, estrone, estradiol, testosterone, testosterone propanoate, β -estradiol 17-acetate, and tetrahydrofuran (THF) were purchased from Aldrich (St. Louis, MO, USA). Ivium potentiostat (Ivium Technologies, Netherlands) was used to obtain the cyclic voltammograms. A round gold plate, which was manufactured at a jewelry store, was used as a working electrode. Its surface area was $1.0\text{ cm}^2 \times 2$, and its thickness was 0.50 mm. The gold plate was cleaned using piranha solution prior to use [23]. The piranha solution was obtained by mixing 30 mL of 30 wt% H_2O_2 and 90 mL of concen-

[†]To whom correspondence should be addressed.

E-mail: yshin@bnl.gov

Copyright by The Korean Institute of Chemical Engineers.

trated sulfuric acid. In the cleaning process, the gold plate was located in the piranha solution for 15 min and later transferred into deionized water for 10 min. It was cleaned with deionized water [23]. ACE-200 spin coater (Dong Ah Trade Co., Korea) was used for spin coating. Horiba Uvisel 2 Ellipsometer. (Kyoto, Japan) was used to measure the coating thickness.

2. SAM Formation on the Surface of the Au Plate

The gold plate was immersed in a solution containing the thiol compound for 12 h to form the SAM on the gold plate. The solution containing the thiol compound was prepared with 198 mg (1.80 mmol) benzenethiol and 25.2 mg (0.20 mmol) 4-mercaptophenol in 100 mL ethanol. This gold plate was transferred into 50 mL ethanol for 30 min to remove the overcoated thiol compound. The gold plate was dried under vacuum for 3 h. The process was conducted by hanging the gold plate, and the reaction was carried out on both sides of the plate [23].

3. Reaction of Cholesteryl Chloroformate with 4-Mercaptophenol on the SAM

The gold plate with the SAM was transferred into the solution containing 1 mL triethylamine in 30 mL dry THF. The solution containing 1.50 g (3.34 mmol) cholesteryl chloroformate in 15 mL THF was added in the above solution with stirring. The solution was stirred for 6 h after the solutions were combined. The gold plate was rinsed with THF twice [26].

4. Purification of PMMA and Spin Coating of PMMA on the Gold Plate

The remaining polymerization additives and the low molecular weight PMMA were removed as follows. First, 1.0 g PMMA (M_w 350,000) was dissolved in 20 mL acetone. This solution was added dropwise to 100 mL methanol with stirring. The precipitate was collected, and the dissolution of PMMA in acetone and its dropwise addition to methanol was repeated two more times, so the process was conducted three times totally. The final precipitate was dried under vacuum for 6 h. Using this PMMA material, the spin coating was conducted using the 0.30 wt% PMMA in toluene at 6,000 rpm for 80 s. The coated gold plate was dried under vacuum for 6 h.

5. Formation of Cholesterol-imprinted Site on the Coating Surface

To hydrolyze the carbonate group linking the cholesterol group with the SAM, the PMMA-coated gold plate was transferred into 1 M NaOH in methanol and refluxed for 6 h. After refluxing, the gold plate was rinsed five times with deionized water. The hydrolyzed cholesterol was extracted with methanol and extracted with hexane once more [26].

6. Electrochemical Measurement

The measurement equipment comprised a three-electrode system including a working electrode, a reference electrode, and a counter electrode in 50 mL reactor. Cholesterol-imprinted gold plate was used as a working electrode. The 10 cm platinum wire was used as a counter electrode and Ag/AgCl (3 M KCl) was used as a reference electrode [26].

During the electrochemical measurement, the redox reaction of potassium ferricyanide was used as a background reaction [23]. It was carried out with 5.0 mM potassium ferricyanide and 50 mM sodium perchlorate composed of 0.0495 g (0.150 mmol) potassium

ferricyanide and 0.1838 g (1.50 mmol) sodium perchlorate in the mixed solvent containing 15 mL ethanol and 15 mL distilled water. The cyclic voltammogram was measured between -0.5 V and 0.5 V at 50 mV/s. The recognition was measured by estimating the maximum current in the background oxidation reaction by adding cholesterol or cholesterol analogs. A 1.0 mM solution of cholesterol or cholesterol analogs was prepared, and supplemented with 150 μ L solution every time, i.e., the concentration of the solution was increased 5 μ M per addition.

7. Formation of Non-imprinted Electrode

The non-imprinted electrode was designed to compare experimental outcome with cholesterol-imprinted electrode. The same gold plate was used to form the SAM with the same thiol compound solution. The same PMMA solution was coated on this SAM. Comparing the formation process of the non-imprinted electrode with that of the cholesterol-imprinted electrode, the reaction step of cholesteryl chloroformate and the hydrolysis step of carbonate group were omitted.

RESULTS AND DISCUSSION

1. Formation of Cholesterol-imprinted Site on SAM

Molecular imprinting involves covalent and non-covalent bonding methods. In the covalent bonding method, covalent bonding exists between the target molecule and the polymeric material. Generally, non-covalent bonding method is used because of its simplicity compared with covalent bonding. However, covalent bonding can generate a more elaborate molecular imprinted site. The covalent bonding method was used in this study. The surface molecular imprinting technique was also used. Cholesterol imprinting was conducted on the round gold plate. The SAM was formed using benzenethiol and 4-mercaptophenol at a molar ratio of 9 : 1. Previous studies showed that this ratio yielded the most superior cholesterol recognition because of the maximum formation of molecular imprinting sites isolated independently [26]. After the SAM formation, the reaction between cholesteryl chloroformate and hydroxyl group in 4-mercaptophenol linked the cholesterol to the SAM via covalent bonding. The PMMA coating enveloped the cholesterol group. Under this state, the optimum coating thickness is very important to facilitate the hydrolysis and extraction of cholesterol. In our previous study [26], the coating thickness was unsuccessfully controlled, and therefore, after the coating, the partial exfoliation method was used to control the thickness. Partial exfoliation involved the leaving and the stroking methods. The stroking method yielded better results compared with the leaving method. However, the results of the stroking method were partly dependent on the investigators. Therefore, we searched for the direct coating conditions to obtain the optimum coating thickness without partial exfoliation in this study. We finally determined that the viscosity of the solution was the most important condition in minimizing the coating thickness. In this study, we selected the PMMA with an M_w 350,000 instead of the PMMA with M_w 120,000, which was used in the previous study [26]. Using the PMMA with an M_w 350,000, the removing process of the remaining additives during the polymerization was conducted. In this process, the low-molecular weight PMMA was also removed. The PMMA was dissolved in acetone

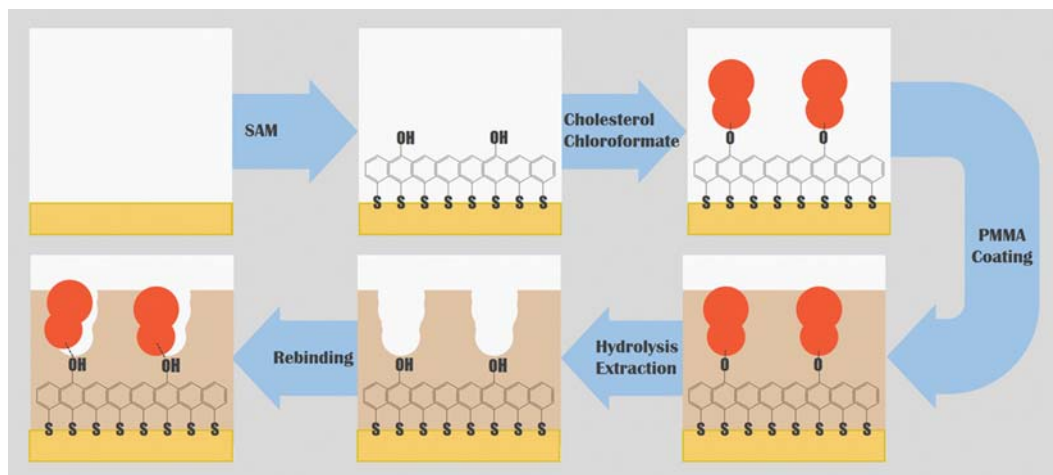


Fig. 1. A schematic diagram of cholesterol imprinting process.

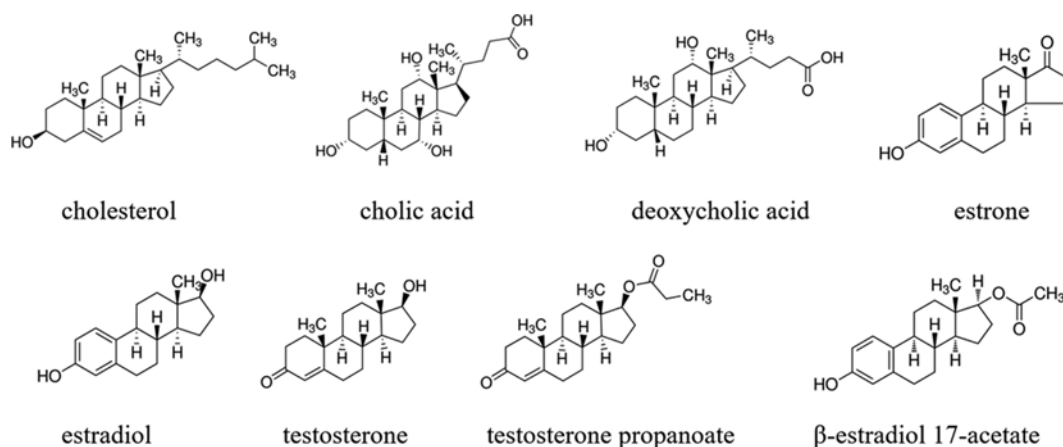


Fig. 2. Chemical structures of cholesterol analogs used in this study.

and precipitated in methanol. This process was repeated three times for the removal. After the removal, the molecular weight was increased to 375,000. Using the PMMA obtained, the coating was performed with 0.30 wt% in toluene solution at 6,000 rpm for 80 s. After drying under vacuum, the coating thickness was 3.2 ± 0.2 nm.

The hydrolysis reaction was conducted and the hydrolyzed cholesterol was extracted using the solvent. Finally, the cholesterol-imprinted site was formed and used for cholesterol recognition. The process is outlined in Fig. 1.

2. Recognition Ability Estimation of the Cholesterol-imprinted Site

We estimated the recognition potential of our system by comparing seven cholesterol analogs. The chemical structures of cholesterol and the seven cholesterol analogs are shown in Fig. 2.

Using the cholesterol-imprinted gold plate as a working electrode, the maximum current was estimated during the background oxidation reaction. The reduced maximum current values were estimated at every $5 \mu\text{M}$ increase in the cholesterol or the cholesterol analogs until $35 \mu\text{M}$. The large amount of the reduced value indicates the exquisite fit of the added molecule with the cholesterol-imprinted site. The results are shown in Fig. 3(a). Using the non-

imprinted gold plate as a working electrode, the results of the above experiment are shown in Fig. 3(b).

In Fig. 3(a) with a cholesterol-imprinted electrode, cholesterol shows the largest current reduction compared with the results of cholesterol analogs. The order of the current reduction was cholesterol >> testosterone propanoate > β -estradiol 17-acetate > estrone = testosterone > estradiol > deoxycholic acid > cholic acid. As shown in Fig. 3(b), using a non-imprinted electrode similar low values were obtained for all the cholesterol analogs including cholesterol.

To accurately estimate the recognition ability, the imprinting factor and the selectivity factor were estimated using the reduced current value at $30 \mu\text{M}$. The imprinting factor was estimated using the following equation:

$$\text{Imprinting factor} = \text{Red}_{MI} / \text{Red}_{NI}$$

Red_{MI} denotes the reduced current, which was detected with $30 \mu\text{M}$ of cholesterol or its analogs using a cholesterol-imprinted electrode, and Red_{NI} refers to the reduced current, which was detected at $30 \mu\text{M}$ of cholesterol or its analogs using a non-imprinted electrode. The imprinting factor indicates the efficiency of the cholesterol-imprinted electrode compared with the non-imprinted electrode. The selec-

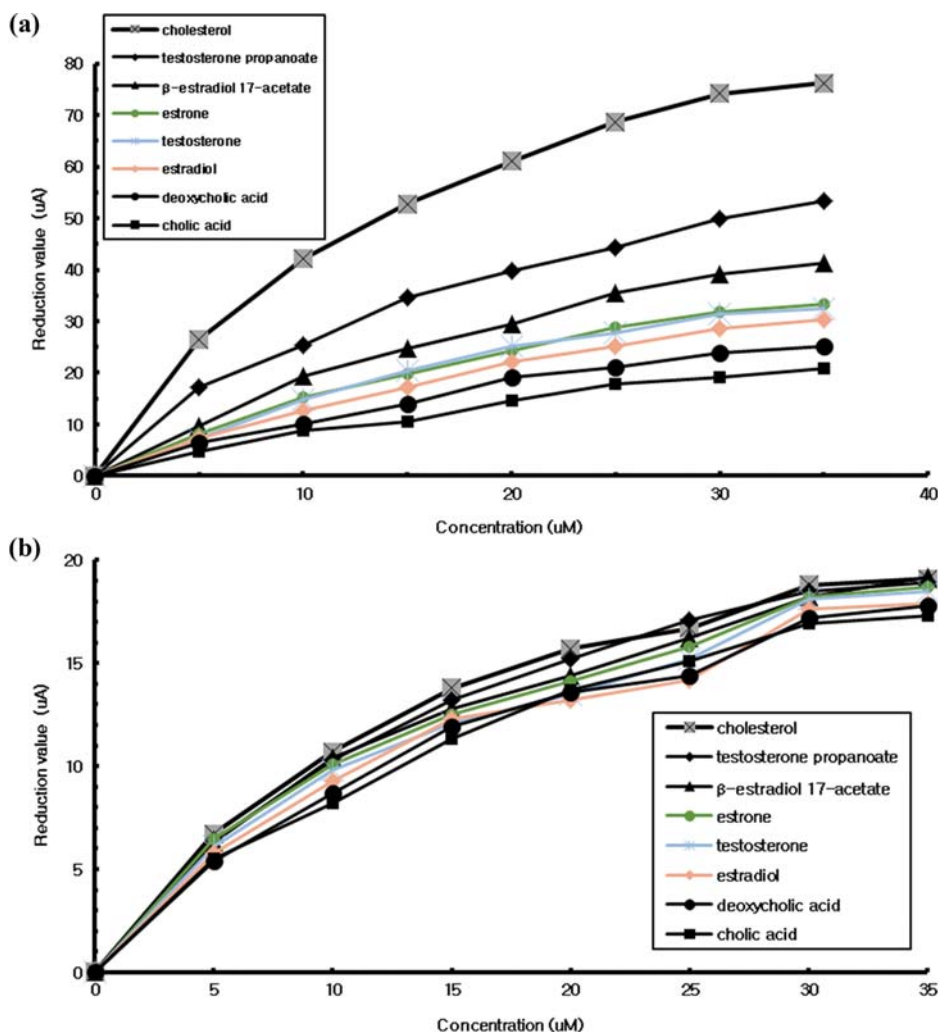


Fig. 3. Current reduction value in the cyclic voltammogram of cholesterol and cholesterol analogs addition. (a) cholesterol-imprinted electrode, (b) non-imprinted electrode.

Table 1. The imprinting and the selectivity factors for cholesterol and its analogs

	Red_{MI}	Red_{NI}	ΔRed	Imprinting factor	Selectivity factor
Cholesterol	74.2	18.8	55.4	3.95	1
Cholic acid	19.2	16.9	2.3	1.14	0.042
Deoxycholic acid	23.8	17.2	6.6	1.38	0.12
Estrone	31.3	18.1	13.1	1.73	0.24
Estradiol	28.5	17.6	10.9	1.62	0.20
Testosterone	31.8	18.2	13.6	1.75	0.25
Testosterone propanoate	49.8	18.5	31.3	2.69	0.56
β -Estradiol 17-acetate	39.1	18.2	20.9	2.15	0.38

tivity factor is obtained from the relative value of ΔRed , ($Red_{MI} - Red_{NI}$) using the data of cholesterol and its analogs. The selectivity factor is estimated using the following equation:

$$\text{Selectivity factor} = \Delta Red_{\text{analog}} / \Delta Red_{\text{cholesterol}}$$

$\Delta Red_{\text{analog}}$ denotes the difference between Red_{MI} and Red_{NI} in the cholesterol analogs, and $\Delta Red_{\text{cholesterol}}$ refers to the gap between Red_{MI}

and Red_{NI} for the cholesterol. The selectivity factor indicates the segregation ratio of the cholesterol analogs to cholesterol.

The results of the imprinting factor and the selectivity factor are shown in Table 1.

In Table 1, the imprinting factor indicates the relative reduction of the cholesterol-imprinted electrode compared with the non-imprinted electrode. In the case of cholesterol, the imprinting factor

was 3.95, which was the largest value among the eight compounds in this study, and in case of cholic acid, it was 1.14, which was the lowest value. The selectivity factor of cholic acid in Table 1 was 0.042, which is also the lowest value among the cholesterol analogs. The selectivity may be attributed to two additional hydroxyl groups and one carboxyl acid group in the cholic acid compared with cholesterol. In case of deoxycholic acid, it has one reduced hydroxyl group compared with cholic acid. Therefore, deoxycholic acid showed a minor increase in selectivity compared with cholic acid. However, deoxycholic acid still showed a lower selectivity factor because it carries an additional hydroxyl group and a single carboxyl acid group compared with cholesterol. Estrone showed a larger selectivity factor than estradiol. Estrone contains a ketone group instead of hydroxyl group in estradiol. Testosterone showed similar selectivity factor compared with estrone.

β -Estradiol 17-acetate showed a higher selectivity factor than estradiol because β -estradiol 17-acetate carries an alkyl side chain even though it is very short. This effect was observed more clearly for testosterone propanoate, which showed higher selectivity than any other cholesterol analogs. Especially, it exhibited a higher selectivity factor than testosterone. Its selectivity factor of 0.56 suggests structural similarity with cholesterol. Conclusively speaking, the order of the selectivity factor was cholesterol >> testosterone propanoate > β -estradiol 17-acetate > testosterone = estrone > estradiol > deoxycholic acid > cholic acid. A very low selectivity factor results in segregation of the compound by the sensing system to cholesterol. In case of compounds with very high selectivity factor, the sensing system cannot segregate them to cholesterol, suggesting that the system cannot segregate the compound to cholesterol because of similar chemical structures.

CONCLUSIONS

Molecular imprinting was conducted on the thin polymeric membrane of the SAM with cholesterol as the target compound. The recognition ability was estimated by measuring the maximum current in the background oxidation reaction using a cholesterol-imprinted electrode. Results of the seven cholesterol analogs were compared with cholesterol. The imprinting and selectivity factors were estimated using the data at 30 μ M concentration. The imprinting factor was 3.95 for cholesterol, suggesting satisfactory performance of the cholesterol-imprinted site. The selectivity factor of cholic acid was 0.042, which was the lowest value. It suggested that the cholesterol-imprinted site segregated cholic acid adequately. The selectivity factor of testosterone propanoate was 0.56, which was a relatively higher value indicating that testosterone propanoate has a very similar chemical structure and polarity compared to cholesterol. The cholesterol-imprinted system was developed at the thin polymeric membrane on SAM to improve the molecular imprinting method, and the system was characterized in detail in this study.

ACKNOWLEDGEMENT

This research was supported by the Basic Science Research Pro-

gram funded by the National Research Foundation (NRF) of Korea (NRF-2017R1C1B5015673 for Min Jae Shin).

REFERENCES

1. Y. Zhang, E. Vittinghoff, M. J. Pletcher, N. B. Allen, A. Z. Hazzouri, K. Yaffe, P. P. Balte, A. Alonso, A. B. Newman, D. G. Ives, J. S. Rana, D. Lloyd-Jones, R. S. Vasani, K. Bibbins-Domingo, H. C. Gooding, S. D. Ferranti, E. C. Oelsner and A. E. Moran, *J. Am. Coll. Cardiol.*, **74**, 330 (2019).
2. V. Narwal, R. Deswal, B. Batra, V. Kalra, R. Hooda, M. Sharma and J. S. Rana, *Steroids*, **143**, 6 (2019).
3. N. K. Chua, G. Hart-Smith and A. J. Brown, *J. Biol. Chem.*, **294**, 8134 (2019).
4. S. Kumar, B. K. Kaushik, R. Singh, N. K. Chen, Q. S. Yang, X. Zhang, W. Wang and B. Zhang, *Biomed. Opt. Express.*, **10**, 2150 (2019).
5. A. Panja and K. Ghosh, *Supramol. Chem.*, **31**, 239 (2019).
6. J. Dong, X. Du, H. Wang, J. Wang, X. Chen, Z. Zhu, Z. Luo, L. Yu, A. J. Brown, H. Yang and J. W. Wu, *Nat. Commun.*, **10**, 829 (2019).
7. K. Pramanik, P. Sarkar, D. Bhattacharyay and P. Majumdar, *Electroanal.*, **30**, 2719 (2018).
8. K. C. Courtney, K. Y. Fung, F. R. Maxfield, G. D. Fairn and X. Zha, *eLife*, **7**, 38493 (2018).
9. J. J. BelBruno, *Chem. Rev.*, **119**, 94 (2019).
10. S. P. Mtolo, P. N. Mahlambi and L. M. Madikizela, *Water Sci. Technol.*, **79**, 356 (2019).
11. R. D. Crapnell, A. Hudson, C. W. Foster, K. Eersels, B. Grinsven, T. J. Cleij, C. E. Banks and M. Peeters, *Sensors*, **19**, 1204 (2019).
12. M. Zarejousheghani, W. Lorenz, P. Vanninen, T. Alizadeh, M. Cammerer and H. Borsdorf, *Polymers*, **11**, 888 (2019).
13. A. H. Kamel, S. G. Mohammad, N. S. Awwad and Y. Y. Mohammed, *Int. J. Electrochem. Sci.*, **14**, 2085 (2019).
14. P. X. M. Rangel, S. Laclef, J. Xu, M. Panagiotopoulou, B. Kovensky, B. T. S. Bui and K. Haupt, *Sci. Rep.*, **9**, 3923 (2019).
15. Z. Zhang and J. Liu, *Small*, **15**, 1805246 (2019).
16. M. Sobiech, P. Bujak, P. Lulinski and A. Pron, *Nanoscale*, **11**, 12030 (2019).
17. A. A. H. Bukhari, M. Minier and N. H. Elsayed, *Polym. Int.*, **68**, 1460 (2019).
18. L. Wang, K. Zhi, Y. Zhang, Y. Liu, L. Ahang, A. Yasin and Q. Lin, *Polymers*, **11**, 602 (2019).
19. S. Ansari and S. Masoum, *TrAC Trends Anal. Chem.*, **114**, 29 (2019).
20. D. H. Yang, M. J. Shin, K. Kim, Y. D. Kim, H. Kim and J. S. Shin, *Microchim. Acta*, **183**, 1601 (2016).
21. M. J. Shin, Y. J. Shin, S. W. Hwang and J. S. Shin, *Int. J. Polym. Sci.*, **2013**, 290187 (2013).
22. M. J. Shin, Y. J. Shin and J. S. Shin, *Open J. Org. Polym. Mater.*, **3**, 1 (2013).
23. M. J. Shin and W. H. Hong, *Biochem. Eng. J.*, **54**, 57 (2011).
24. M. J. Shin, Y. J. Shin and J. S. Shin, *Part. Sci. Technol.*, **30**, 543 (2012).
25. M. J. Shin, Y. J. Shin and J. S. Shin, *J. Ind. Eng. Chem.*, **20**, 91 (2014).
26. M. J. Shin, Y. J. Shin and J. S. Shin, *Colloids Surf., A*, **559**, 365 (2018).
27. M. J. Shin, M. Kim and J. S. Shin, *Polym. Int.*, **68**, 1722 (2019).